

RESEARCH

Open Access



# Marine DNA methylation patterns are associated with microbial community composition and inform virus-host dynamics

Hoon Je Seong<sup>1</sup>, Simon Roux<sup>2</sup>, Chung Yeon Hwang<sup>3</sup> and Woo Jun Sul<sup>1\*</sup>

## Abstract

**Background:** DNA methylation in prokaryotes is involved in many different cellular processes including cell cycle regulation and defense against viruses. To date, most prokaryotic methylation systems have been studied in culturable microorganisms, resulting in a limited understanding of DNA methylation from a microbial ecology perspective. Here, we analyze the distribution patterns of several microbial epigenetics marks in the ocean microbiome through genome-centric metagenomics across all domains of life.

**Results:** We reconstructed 15,056 viral, 252 prokaryotic, 56 giant viral, and 6 eukaryotic metagenome-assembled genomes from northwest Pacific Ocean seawater samples using short- and long-read sequencing approaches. These metagenome-derived genomes mostly represented novel taxa, and recruited a majority of reads. Thanks to single-molecule real-time (SMRT) sequencing technology, base modification could also be detected for these genomes. This showed that DNA methylation can readily be detected across dominant oceanic bacterial, archaeal, and viral populations, and microbial epigenetic changes correlate with population differentiation. Furthermore, our genome-wide epigenetic analysis of *Pelagibacter* suggests that GANTC, a DNA methyltransferase target motif, is related to the cell cycle and is affected by environmental conditions. Yet, the presence of this motif also partitions the phylogeny of the *Pelagibacter* phages, possibly hinting at a competitive co-evolutionary history and multiple effects of a single methylation mark.

**Conclusions:** Overall, this study elucidates that DNA methylation patterns are associated with ecological changes and virus-host dynamics in the ocean microbiome.

**Keywords:** Ocean microbiome, DNA methylation, Metagenome-assembled genome, Host–phage, Long-read sequencing

## Background

DNA methylation is an important epigenetic modification that is involved in prokaryotic processes such as gene expression regulation, virulence, DNA mismatch repair, and cell-cycle regulation [1, 2]. While there has been increasing interest in the role of prokaryotic methylation

systems in bacterial genetics, physiology, and ecology, the function and implications of prokaryotic methylation systems in environmental conditions are poorly understood. This is primarily because previous research has focused extensively on culturable prokaryotes, whereas the majority of environmental bacteria are currently not culturable under laboratory conditions.

In prokaryotes, DNA methylation has been largely associated with restriction-modification (RM) systems, which protect host cells against invasion by viruses or against horizontal gene transfer of extracellular DNA by

\*Correspondence: sulwj@cau.ac.kr

<sup>1</sup> Department of Systems Biotechnology, Chung-Ang University, Anseong, Republic of Korea

Full list of author information is available at the end of the article



distinguishing host DNA from sequence-specific DNA methylation [3]. Furthermore, DNA methyltransferase (MTases) that methylate nucleotides without cognate restriction enzymes (REases) are referred to as orphan MTases. Some well-studied orphan MTases play important physiological roles beyond RM systems, including transcriptional regulation and cell phenotype variations [1, 2, 4, 5].

The advent of long-read sequencing technology has opened a new era in methylation research and has enabled the identification of chemical modifications in the DNA structure. Nanopore sequencing enables the identification of all known base modifications [ $N^6$ -methyladenosine ( $m^6A$ ),  $N^4$ -methylcytosine ( $m^4C$ ), and  $N^5$ -methylcytosine ( $m^5C$ )], whereas the ability of single-molecule real-time (SMRT) sequencing to identify these modifications remains currently limited [6]. Conversely, SMRT sequencing can identify DNA methylation at a single-nucleotide resolution, whereas nanopore sequencing has limitations in detecting accurate modification signals due to current level noise [6]. In the metagenomic perspectives, this methylation information has been used in the past to improve prokaryotic genome binning [7, 8]. However, outside these few examples, few attempts have been made to apply long-read metagenomic sequencing to detect DNA methylation directly in the environmental microbiome [9], and link methylation patterns to ongoing eco-evolutionary processes.

Here, we applied meta-epigenomic analysis to genome-centric metagenomics of the open ocean microbial communities in the northwest Pacific Ocean to reveal the role of DNA methylation in environmental microbial communities. Specifically, we explored how molecular mechanisms for base methylation changed in frequency and patterns across taxa and genomes, both across entire communities and within individual populations, and investigated whether these changes could be associated with cell regulation mechanisms and/or inter-organismal interactions. We report that the DNA methylome is differentiated by taxonomic lineage and is affected by the complexity of the community, i.e., the co-existence of multiple closely related strains. We further link methylation patterns to cell cycle regulation and phage defense for *Pelagibacter* genomes, highlighting the multiple roles played by DNA methylation in one of the dominant bacteria of the marine environment.

## Results

### Novel microbial genomes from the northwest Pacific Ocean metagenome

In the 2015 Shipborne Pole-to-Pole Observations (SHIPPO) project of the Korea Polar Research Institute, we conducted shotgun metagenomic sequencing

using ocean surface samples from 10 stations (referred to as St2–St11) by traveling about 4000 km from the Pacific Northwest to the Bering Sea during July 22–29, 2015 (Supplementary Figure S1, Supplementary Table S1). To capture free-living organisms, we extracted genomic DNA after 0.22–1.6- $\mu$ m size filtering, followed by metagenomic sequencing using short- and long-read sequencers. Extensive computational analysis was performed on all samples to reconstruct the genomes across the kingdom using a combination of individual, co-, and hybrid assembly, binning, and refinement methods (Fig. 1). This strategy allowed the recovery of a total of 15,056 viral, 252 prokaryotic, 56 giant viral, and 6 eukaryotic metagenome-assembled genomes (MAGs, specifically referred to here as SHIPPO vMAGs, proMAGs, gvMAGs, and eukMAGs, respectively; Supplementary Data 1 and 2). These proMAGs mainly consist of the bacterial phyla of Proteobacteria ( $n = 120$ ), Bacteroidota ( $n = 88$ ), Actinobacteriota ( $n = 11$ ), and the archaeal phyla of Thermoplasmatota ( $n = 15$ ) (Fig. 2a).

Short- and long-read assembly and binning strategy substantially improved the fraction of mapped metagenomic reads. Overall, the average mappability of all samples was 38.03% (std. 2.88) (Supplementary Figure S2). Most of the reads mapped to vMAGs and proMAGs, with relatively smaller representation of gvMAGs and eukMAGs. We compared our proMAGs with the *Tara* [10] and Global Ocean Reference Genomes Tropics (GORG-Tropics) [11] datasets to evaluate the novelty of our recovered genomes (Fig. 2b). Although these proMAGs and single-cell amplified genomes datasets came from a global-scale study [10, 11], only three proMAGs overlapped at the species level ( $\geq 95\%$  ANI) with our proMAGs. Furthermore, 95% of the proMAGs obtained here could not be classified at the species level, even though the Genome Taxonomy Database (GTDB) [12] includes genomes of uncultured organisms derived from shotgun metagenomics and single-cell genomics. Thus, despite previous extensive ocean metagenomic binning efforts such as those undertaken on data from mega-surveys like the *Tara* Ocean Expedition [10] and the Global Ocean Survey [11], the northwest Pacific Ocean datasets from this study provide substantial novel genomic information on ocean microbiomes.

### DNA MTases in marine microorganisms

To characterize the role of MTases in ocean microbial communities, we first identified the type of MTases and their cognate REases distribution from the genome catalog established here and derived from previous ocean microbiome surveys (GORG, TARA, and SHIPPO). Of the total 5713 medium-quality proMAGs, we found 67.18% (3838) and 19.45% (1111) of proMAGs encoded

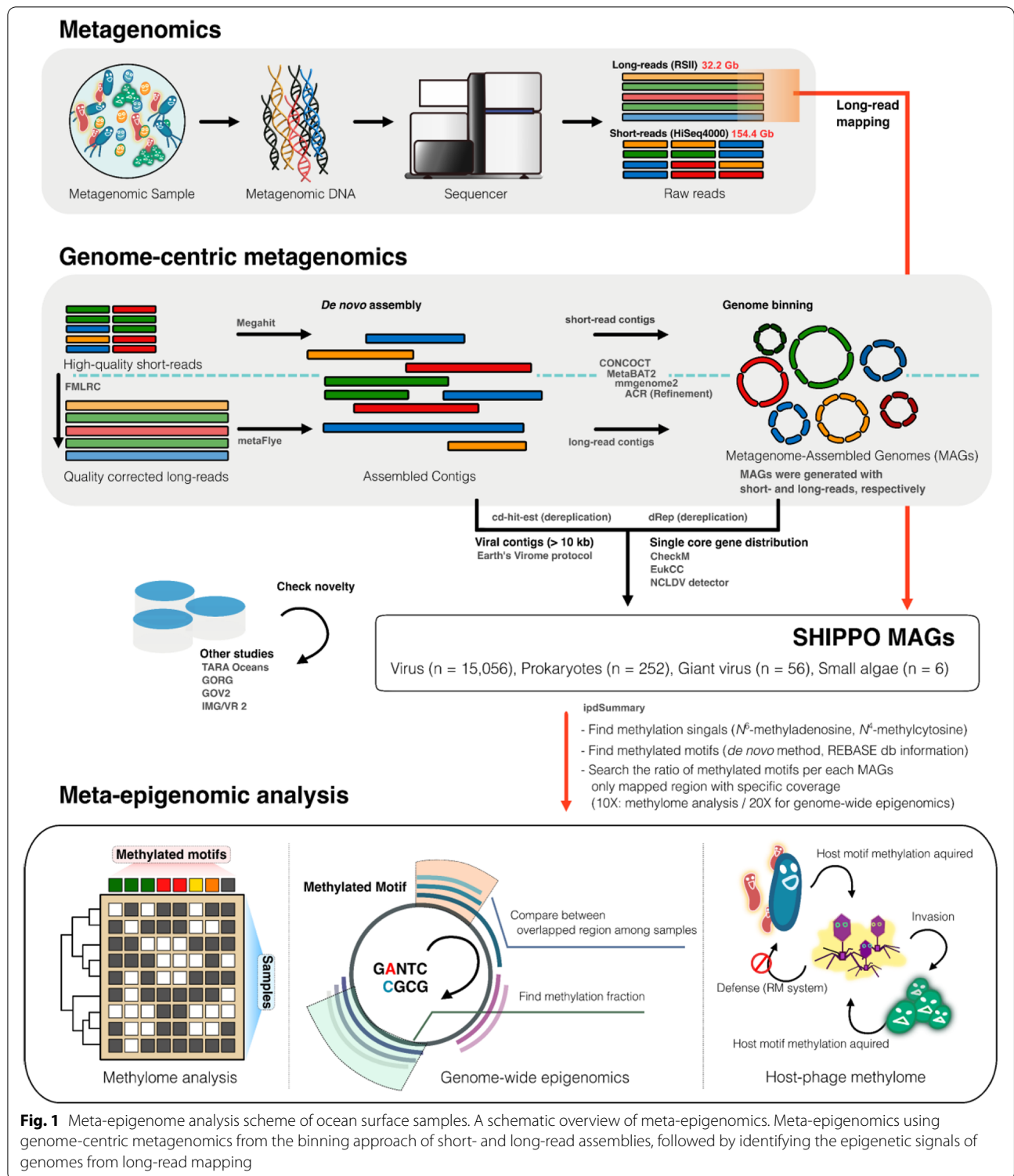
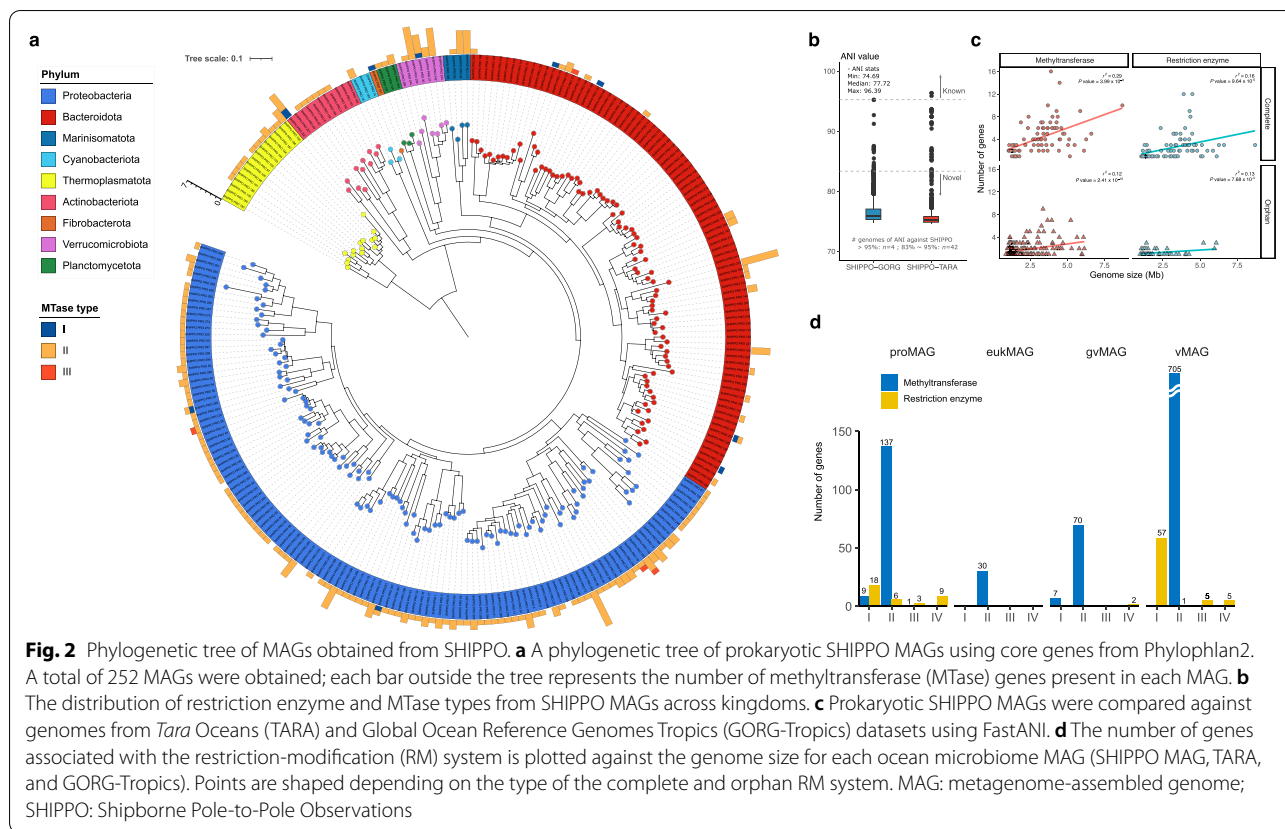


**Fig. 1** Meta-epigenome analysis scheme of ocean surface samples. A schematic overview of meta-epigenomics. Meta-epigenomics using genome-centric metagenomics from the binning approach of short- and long-read assemblies, followed by identifying the epigenetic signals of genomes from long-read mapping

one or more MTases and REases, respectively (Supplementary Data 3). Among the four MTase types—I, II, III, and IV—type II MTase was found most frequently (94.71%) in proMAGs with MTases, followed by type

I (14.02%) and III (2.16%). Of all the proMAGs, only 14.77% had a complete RM system; most consisted of type I and III MTases: 76.39% and 74.70% of type I and III MTases constituted a complete RM system, respectively,



whereas only 3.19% of type II MTases constituted an RM system. By contrast, most MTases (86.09%) belonged to orphan MTases, thus lacking counterpart REases, and consisted of type II MTases. To compare the genome size of ocean prokaryotes and the number of genes related to RM systems, 424 near-complete proMAGs were used. Although the number of MTase and REase correlated with genome size, the genome of proMAG with one or more RM system was significantly larger than that of proMAG with orphan MTase (Wilcoxon’s rank-sum  $P$  value  $< 2.2 \times 10^{-16}$ ). In addition, in the case of proMAG with RM system, the correlation between MTase and genome size ( $r^2$  0.29) was higher than for REase ( $r^2$  0.16) (Fig. 2c). Overall, in the ocean microbial community, most prokaryotic RM systems suggest being composed of essential cellular mechanisms rather than the defense system. By contrast, type I and III MTases and their cognate REases typically serve as a defense mechanism through the RM system and thus are harbored in genomes of relatively large size.

Beyond MTases detected in proMAGs, a total of 959 MTases were found in the SHIPPO MAGs catalog, including all ( $n = 6$ ) of the eukMAGs, 62.5% ( $n = 35$ ) of the gvMAGs, 36.90% ( $n = 93$ ) of the proMAGs, and 4.28% ( $n = 645$ ) of the vMAGs (Fig. 2d and

Supplementary Data 3). Consistent with the abovementioned results, type II MTases were the most frequently detected for all domains (Fig. 2d). All but two MTases were solitary or orphan MTases that have no counterpart REases. Eukaryotes and giant viruses had an average of 5.0 and 2.2 MTases per genome, whereas fewer MTases were found in the prokaryotic and viral genomes (1.58 and 1.09 per genome, respectively).

### DNA methylome of SHIPPO MAGs

We next studied the DNA methylation patterns of the ocean microbiome and compared DNA methylation profiles of each SHIPPO MAG across samples. We first performed a principal coordinate analysis (PCoA) based on the Kulczynski dissimilarity of 5-mer DNA methylation profiles for individual MAG-sample pairs (requiring  $10\times$  coverage with 20% genome breadth for proMAGs and gvMAGs, 10% for eukMAGs, and 60% for vMAGs; Supplementary Data 4). DNA methylation profiles were grouped clearly by domain, i.e., separating eukaryotes, prokaryotes, and virus MAGs (Fig. 3a). In particular, Alphaproteobacteria harbored distinct methylation profiles compared to all other microbial organisms, and Alphaproteobacteria proMAGs were partitioned from each other down to the family level.

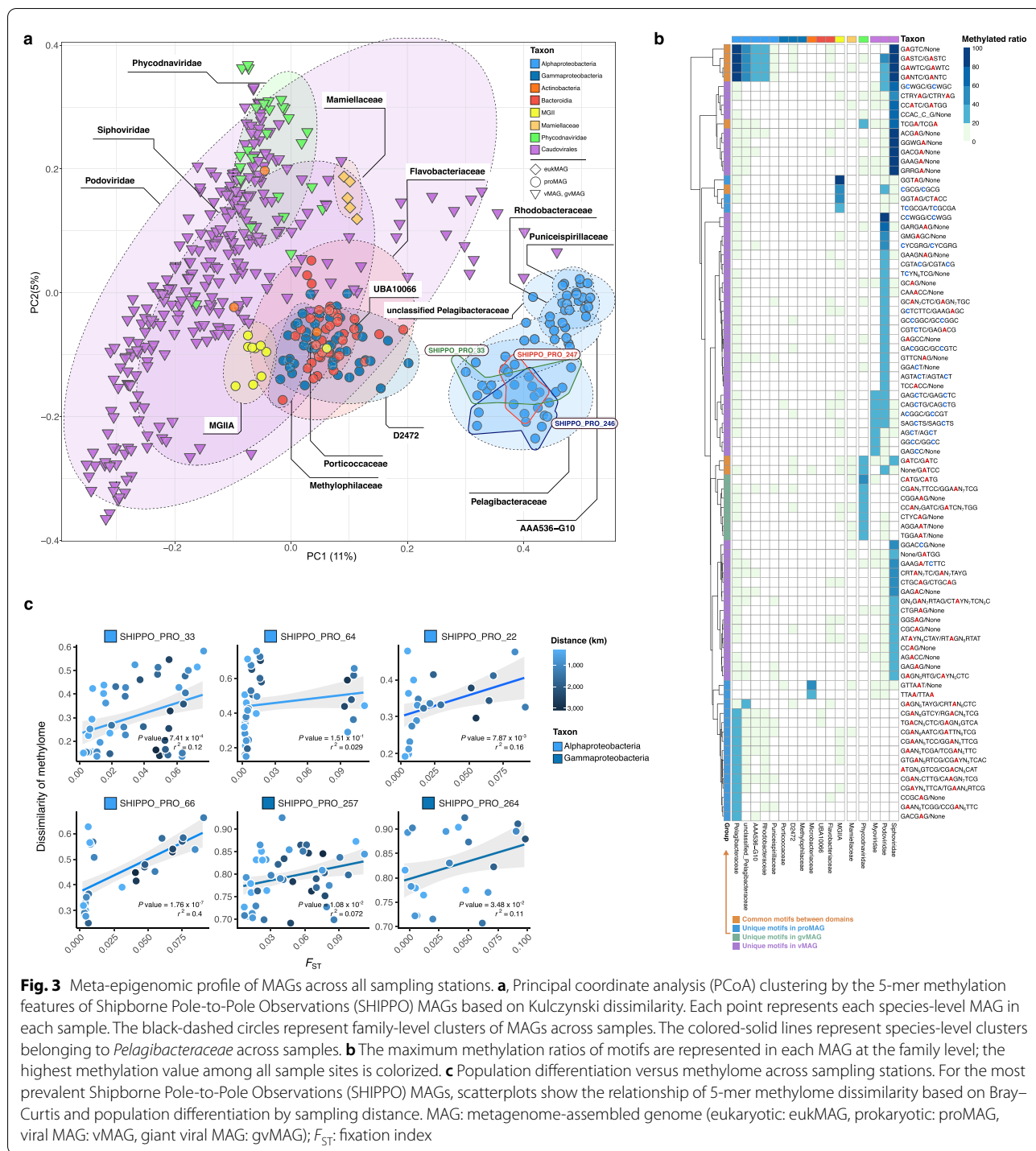


**Fig. 3** Meta-epigenomic profile of MAGs across all sampling stations. **a**, Principal coordinate analysis (PCoA) clustering by the 5-mer methylation features of Shipborne Pole-to-Pole Observations (SHIPPO) MAGs based on Kulczynski dissimilarity. Each point represents each species-level MAG in each sample. The black-dashed circles represent family-level clusters of MAGs across samples. The colored-solid lines represent species-level clusters belonging to *Pelagibacteraceae* across samples. **b** The maximum methylation ratios of motifs are represented in each MAG at the family level; the highest methylation value among all sample sites is colored. **c** Population differentiation versus methylome across sampling stations. For the most prevalent Shipborne Pole-to-Pole Observations (SHIPPO) MAGs, scatterplots show the relationship of 5-mer methylome dissimilarity based on Bray–Curtis and population differentiation by sampling distance. MAG: metagenome-assembled genome (eukaryotic: eukMAG, prokaryotic: proMAG, viral MAG: vMAG, giant viral MAG: gvMAG);  $F_{ST}$ : fixation index

However, the methylation profile of 5-mers could not be distinguished at the species level, as in the example of the *Pelagibacteraceae* cluster, which consisted of SHIPP\_PRO\_33, SHIPP\_PRO\_245, and SHIPP\_PRO\_247. Furthermore, proMAGs belonging to Flavobacteriia, Actinobacteria, Gammaproteobacteria, and

Bacteroidia were also difficult to distinguish by their methylation profile.

To identify the exact DNA methylated motif, the methylated motif information was collected via the Restriction Enzyme database (REBASE) [13]. Although additional motifs were discovered from the *de novo* motif finding

algorithm MultiMotifMaker [14] across SHIPPO MAGs, most motifs were discovered in previous studies (GATC, GANTC, CGCG, VATB, underlining indicates methylation position) [15, 16]. A total of 1357 motifs were searched along the mapped region of each SHIPPO MAG. When < 20% of each motif was methylated in each genome, it was considered noise and excluded from the candidate methylation motifs. Ninety-five candidate methylated motifs were detected, of which 17 and 76 represented m<sup>4</sup>C and m<sup>6</sup>A modifications, respectively. The other two were non-palindromic motifs (CGTCTC/GAGACG, GAAGA/TCCTC) with both m<sup>4</sup>C and m<sup>6</sup>A methylation. Among the methylated motifs, 13 motifs were shared across domains. GANTC was found most frequently in several families belonging to Alphaproteobacteria and in *Caudovirales* (Fig. 3b). CGCG and GGTAG were detected in both archaeal proMAGs affiliated to MGIIA and *Caudovirales* vMAGs (Fig. 3b). The GATC motif was found in gvMAGs (*Phycodnaviridae*), *Caudovirales*, and unclassified vMAGs (Fig. 3b). In addition, there were methylated motifs unique to vMAGs, such as CCWGG and GGCC, and unique motifs were found in each family, such as TTAA (*Microbacteriaceae*), and TCGCGA (MGIIA) (Fig. 3b). The high diversity of methylated motifs in vMAG suggests the existence of many unknown MTases encoded on prokaryotic and/or viral genomes, and is consistent with a role of viral genome methylation in virus-host arms race.

To match the methylated motifs with MTases of each SHIPPO MAG, candidate MTases were searched against REBASE [13] reference MTases with recognition sequence information. Only the recognition sequences of 12 MTases were known, and except for the recognition sequences of one viral MTase, it was confirmed that the methylated motif sequences were identical to the recognition sequence information (Supplementary Table S2). For example, in the seven Alphaproteobacteria proMAGs, we could identify methylation signals from several motifs, including GANTC, GASTC, GAGTC, and CGANNNNNNAATC, but these were represented by GATNC, for which the congruent recognition sequences of the best similarity reference MTase could be found (Supplementary Table S2). There were four methylation motifs in an archaeal proMAG (SHIPPO\_PRO\_101), and after deduplication, two different motifs (CGCG and GGTAG) were represented (Supplementary Table S2). One congruent MTase could be found (CGCG) among these two methylation motifs, but no MTase matched the other methylation motif (GGTAG). Although the GGTAG motif was novel in that it is previously unreported, this result limited the confirmation of the archaeal novel methylation system, likely due to the fact that this MAGs does not represent a complete genome. Furthermore,

except for 12 of the 1124 MTases, it was either difficult to identify the methylation profile due to the long-read sequencing depth or the lack of MTase recognition sites in the previous database made it difficult to compare between MTases and motif sequences.

#### DNA methylation patterns within-population genetic diversity

Several studies of bacterial DNA methylome suggested that different bacterial strains have different methylome patterns, even within species [8, 17, 18]. These changes can be caused by the presence of MTases or by phase-variable MTases that respond to changes in the environment [19]. However, microbial DNA methylation changes in complex environments have not yet been measured directly; therefore, we analyzed intra-species DNA methylation variation at the sampling station. The fixation index ( $F_{ST}$ ) was used to compare the similarity in the population differentiation between samples. proMAGs with low base-pair coverage were excluded because the  $F_{ST}$  had to be calculated by the allele frequencies within the species.  $F_{ST}$  was calculated for dominant proMAGs using a mapping region that overlaps at least 40% breadth with 10× depth in all samples with short reads. The dissimilarity of methylomes was calculated by the methylation frequency of 5-mer nucleotides in a genome. Therefore, to compare the DNA methylation changes for different sampling stations, only six species-level proMAGs were fulfilled by the sequencing coverage of long- and short reads. In five of the six proMAGs, DNA methylome differences and population differentiation across samples correlated significantly, regardless of the distance between sampling stations (Pearson correlation,  $P$  value < 0.05; Fig. 3c). A significant correlation was also found in Gammaproteobacteria proMAGs that showed no specific methylated motif (weak methylated motifs ratio < 10%). These results may indicate that when multiple strains with different methylation profiles of motifs are present in the environment, they affect the methylation pattern at the species level.

#### Genome-wide DNA methylome of Pelagibacter in environmental samples

Next, we analyzed the methylation pattern of dominant proMAGs at the single-nucleotide level to investigate in detail the environmental-dependent changes in methylation. Identifying the single-nucleotide-level DNA methylation from a genome-wide perspective required a relatively deeper and wider read coverage. Four proMAGs (SHIPPO\_PRO\_33, SHIPPO\_PRO\_246, SHIPPO\_PRO\_64, and SHIPPO\_PRO\_101) were covered over > 40% of the breadth of the genome at 20× depth

per strand. Of these, only a SHIPPO\_PRO\_33 proMAG affiliated with *Pelagibacter* overlapped at 65.61% of the genome breadth in all 10 samples. The average breadth of the genome coverage with 20× per strand of SHIPPO\_PRO\_33 was 90.93% (std. 7.40). The in-depth overlapped coverage of long-reads enabled a comparison of methylation patterns between samples for this specific *Pelagibacter* proMAG.

To compensate for the lack of sequencing depth in the genome between samples, we focused on the genome-wide epigenetic analysis of the *Pelagibacter* proMAG (SHIPPO\_PRO\_33; 12 contigs; 87.30 completeness, 3.79 contamination). Only the nucleotide positions of the overlapped regions that could measure methylation in all samples were compared. A total of 2,494 GANTC motifs were detected on both strands of the SHIPPO\_PRO\_33 genome, and only 1719 GANTC (68.93%) were included in the overlapped region (the average depth of reads was 112.85×, std. 60.56) for measuring the methylation at 10 sampling stations. The methylation rate of GANTC varied in the range 71.31–94.77% depending on the sample, of which 2.44% (42 sites) remain unmethylated in all samples. In most cases, unmethylated sites were frequently observed in intergenic regions (66.67%), including regulatory regions (16.70%) (Supplementary Table S3). The GANTC position of one of these seven unmethylated positions of the regulatory region contains the *sufE* (K04488) regulatory region of the Suf (sulfur-forming) system. In addition, it was found to be related to genes essential for the cellular mechanism of *Pelagibacter*, particularly heat shock protein (*groEL*) and large subunit ribosomal protein.

The DNA methylation signal at the nucleotide resolution is calculated from the pooled interpulse duration (IPD) ratio in separate molecules for each genomic locus. Due to the often-found epigenetic heterogeneity [20, 21], these aggregated methylation signals indicate the methylation of cell fractions at the nucleotide level (hereafter referred to as methylation fraction). The methylation fraction of GANTCs was observed in heterogeneity across samples, particularly in St6, St8, and St9. The differences in the methylation fractions on nucleotide sites were referred to as single nucleotide methylation variation (SNMV). Compared to other samples, the number of unmethylated motifs was higher in St6, St8, and St9 and showed different SNMV patterns at each nucleotide position (Fig. 4a). By contrast, all samples, except for St6, St8, and St9, had similar SNMVs to each other and were more closely clustered, regardless of latitude (Fig. 4b). For example, pairs St2 and St3, and St10 and St11, distanced geographically by about 20° latitude and 3000 km distance, were grouped closely through PCoA (Fig. 4b). In particular, differences in strain-level

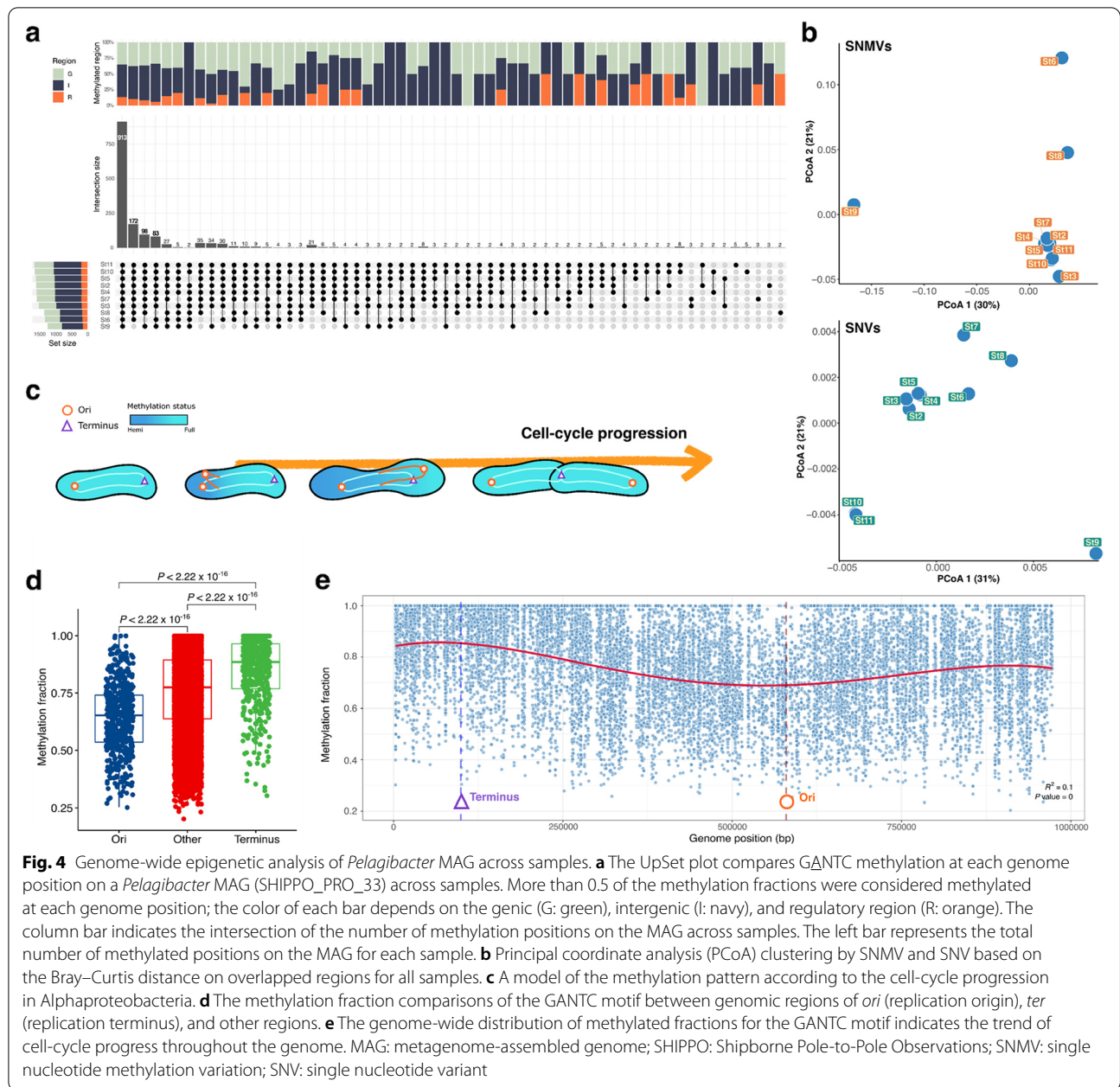
composition (single nucleotide variants; SNVs) were found between these two groups, but in SNMVs, these groups were clustered together (Fig. 4b). These results indicated that DNA methylation at the single nucleotide level differed under environmental conditions regardless of strain composition, which suggests that dynamic cellular events occur among various *Pelagibacter* in northwest Pacific Ocean surface waters.

#### Active replication of *Pelagibacter* relected by MTase activity

Several MTases, such as CcrM, which methylates the GANTC motif, are involved in the cell-cycle regulation in Alphaproteobacteria [22]. When re-analyzing previously published genomic data capturing methylation status of *Cand. P. Giovannoni* NP1 chromosome during exponential growth [23], we noticed a gradual decrease of the genome-wide methylation fraction of GANTC from the replication origin (*ori*) to replication terminus (*ter*) (Supplementary Figure S3). The proposed underlying mechanism [24] is thought to be linked to delayed methylation of the daughter strand: as chromosomal replication proceeds, the methylation status of the parental strand is maintained, whereas GANTC remains unmethylated when a new daughter strand is generated through a replication fork (hemimethylated) (Fig. 4c). As methylases, such as *ccrM* [22], are typically only expressed at the end of chromosome replication, the chromosome remains hemimethylated until the end of replication. When DNA methylation signals are pooled from separate molecules for each genomic locus, the methylation fraction may result in relatively lower values near the *ori* due to the ratio of hemimethylation to full methylation following different DNA replication instances for different cells in the exponential phase (Supplementary Figure 3). The same pattern of a lower methylation fraction in the *ori* region of the chromosome was observed with the *Pelagibacter* proMAG (SHIPPO\_PRO\_33) across several samples under natural environmental conditions (Fig. 4d, e and Supplementary Figure S4). This suggests that some *Pelagibacter* strains are also in an exponential growth phase in natural marine environments, and that GANTC methylation may also be involved in cell cycle regulation for marine *Pelagibacter* strains.

#### DNA methylation of viral genomes

We only observed methylation patterns in 83 vMAGs associated with 67 vOTUs (viral operational taxonomic units) in a total of 15,056 putative viral genomes. The 83 vMAGs grouped into five major lineages based on pairwise genome similarity (Fig. 5a). Most of the clades were composed of vMAGs belonging to the *Caudovirales* order, except for clade V which showed genomic



similarity to high-quality gvMAGs, and is likely composed of genome fragments related to *Phycodnaviridae*. Within the individual clades, there were typically two or three distinct subclades with outgroups, and some methylation patterns were shared between subclades. For instance in clade-III, specific adenine methylation motifs were found within subclades, which were not shared with other clades. Although these subgroups are phylogenetically related, the two different methylated adenine motifs (GRRGA/None and CCATC/GATGG) did not overlap and represent entirely different motif

patterns. Cytosine methylation was dominant throughout clade-II, and methylation was observed in CGCG, GAGCTC, and CYCGRG motifs according to subgroups. On the other hand, both adenine and cytosine methylation were found in clade-IV, and specific methylation was indicated in the GANTC and CCWGG motifs, respectively, depending on the clade. In addition, the methylation in the GATC motif was consistent in clade-I and, together with the motifs found in clades-IV, suggests that it may be associated with bacterial methylation system as a methylation motif frequently



found in Proteobacteria. For clade-V, adenine methylation was detected, as previously reported for *Phycodnaviridae* [25]; in our study, these were found on GATC and CATG motifs. These two methylated motifs were observed spanning genomes belonging to *Phycodnaviridae*, and importantly the same motif has been previously reported in some of their green algae hosts [15].

To investigate how viral methylation patterns are associated with MTase genes, we next evaluated the distribution of MTases according to the phylogenetic distribution of vMAG clades. Of 83 vMAGs, we found only 14 vMAGs encoded MTase genes, all of which belonged to the Type II MTase. Most MTases showed phylogenetic consistency with the vMAGs (Fig. 5b), along with consistencies in the methylated motifs. For instance, four vMAGs in the clade-IIIb, all methylated to the CCATC/GATGG motif were found to encode closely related MTases, yet these MTases had less than 50% similarity to compare within the REBASE. This lack of similarity to characterized MTases was a common observation for vMAG-encoded MTases, and there was thus only one instance of methylated motifs consistent with the predicted recognition sites based on the closest existing MTases, for vOTU\_N\_648 in Clade-I. This suggests that most viral MTase systems are still poorly characterized, and we expect that methylation motifs for these novel MTases could be predicted based on the methylation patterns and phylogenetic distributions of their corresponding vMAGs.

#### Possible implication of methylation in SAR11 phage-host interactions

Most GANTC positions were methylated throughout the *Cand. P. Giovannoni* NP1 genome (Supplementary Figure S3), and this methylation mark is thought to be related to cell cycle regulation (see above). However, uneven methylation patterns were observed in specific regions of the genome due to the lack of GANTC motifs in the proviral region (Fig. 6a). This raised questions about the potential use of the same methylation mark as a defense system, and the evasion of this defense system by pelagiphages (phages infecting SAR11 bacteria) at point in the evolutionary history of the phage-host pairs.

We next reconstructed the phylogeny of 33 publicly available pelagiphage genomes based on a head-tail connector protein and compiled the frequency of GANTC

motifs in the same genomes (Fig. 6b). Surprisingly, about half of the pelagiphage genomes showed a clear depletion in GANTC motif, and the calculated phylogenetic trees clearly showed that the phages clustered according to the density of GANTC motifs in their genome (Fig. 6b, c). This difference was particularly observed in the subfamily *Autographivirinae* of the family *Podoviridae*.

#### Discussion

Several studies have investigated DNA methylation patterns of microorganisms to understand the epigenetic process regulating functional repertoires, virulence, and cell cycle through laboratory cultures. Due to advances in sequencing technology, the epigenome of individual prokaryotes has been studied extensively in recent years, but the overall patterns of direct DNA methylation in the environment has rarely been explored. There are three main reasons why epigenetic studies have not been conducted frequently through metagenomic studies. First, until recently, it was difficult to obtain representative genome from environmental samples due especially to the high diversity of environmental microorganisms. Second, it is still challenging to measure DNA methylation in-depth as it requires relatively expensive long-read sequencing. And finally, there is a lack of pipelines and guidelines for community-wide methylome analysis. To address these limitations, we present here a short-read and long-read hybrid analysis approach yielding high-quality de novo genomes and genomic methylation information at the community scale. Importantly, beyond unique methylation information, the quality-corrected long reads also allowed us to obtain genomes that are difficult to reconstruct otherwise due to high strain diversity, including a novel *Pelagibacter* genome. This analysis framework enables us to describe the distribution and potential biological impacts of DNA methylation in marine microorganisms, that have not been previously interpreted from an environmental perspective.

RM systems are ubiquitous (i.e., they are found in about 90% of the bacterial genomes [27]) and typically act as a defense mechanism to distinguish between self and non-self DNA. However, upon investigating RM system diversity within the ocean microbial communities from the large-scale study of *Tara* Ocean and GORG to our research, complete RM systems were mainly found in RM I and III. In contrast, the type II

(See figure on next page.)

**Fig. 5** DNA methylation of the viral genome. **a** The methylome of 83 prevalent viral Shipborne Pole-to-Pole Observations (SHIPPO) of metagenome-assembled genomes (vMAGs) is indicated by the heatmap with their phylogeny from genome similarities. The star represents vMAGs in **c**. **b** Phylogenetic comparison of the 14 vMAGs harboring MTase and its MTase genes. **c** Changes in vMAG methylation profiles were measured at three sampling stations. Circles represent the methylation ratio of each motif, and bars represent the read mapping breadth of viral genomes with 10× depth

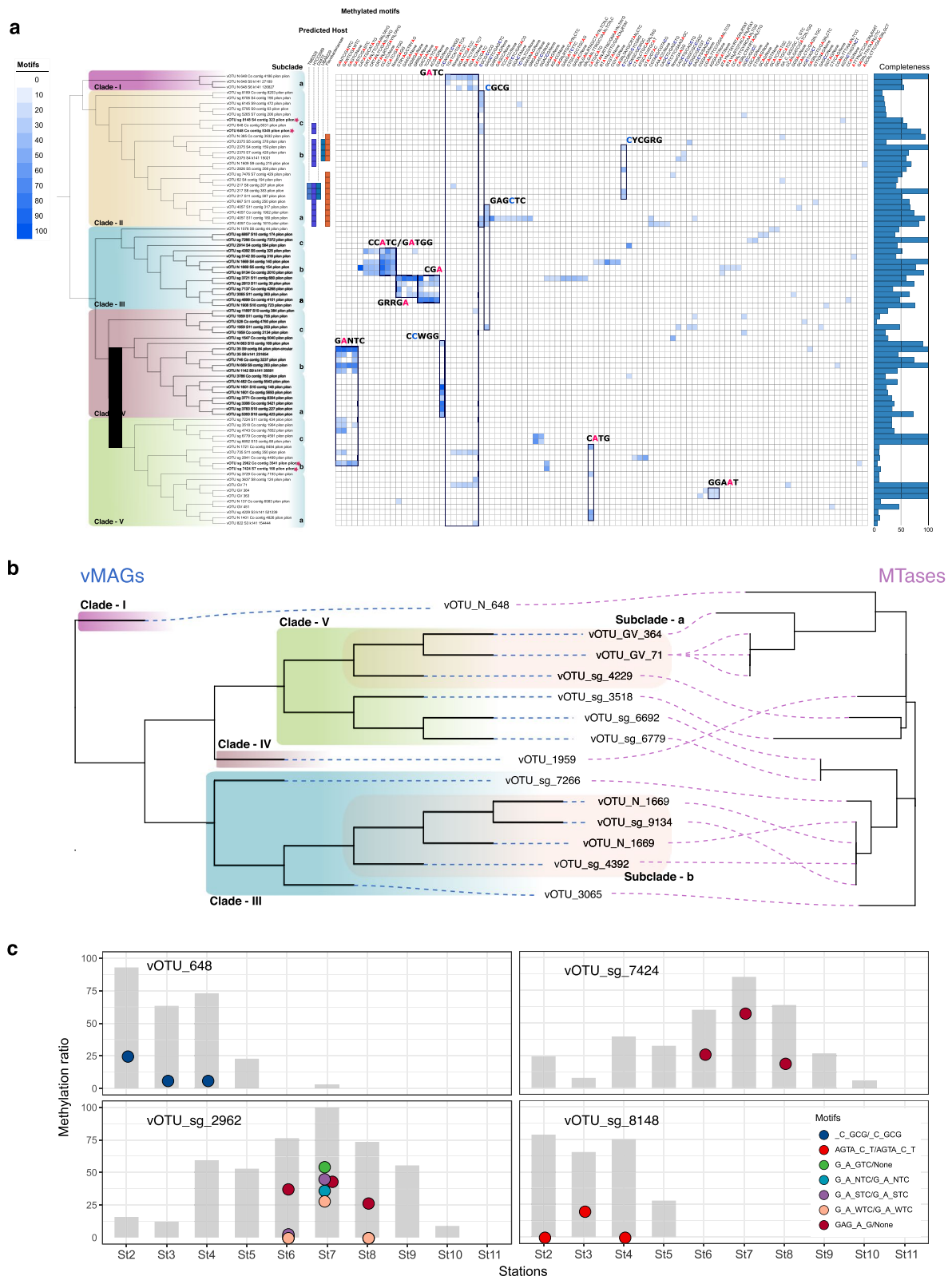
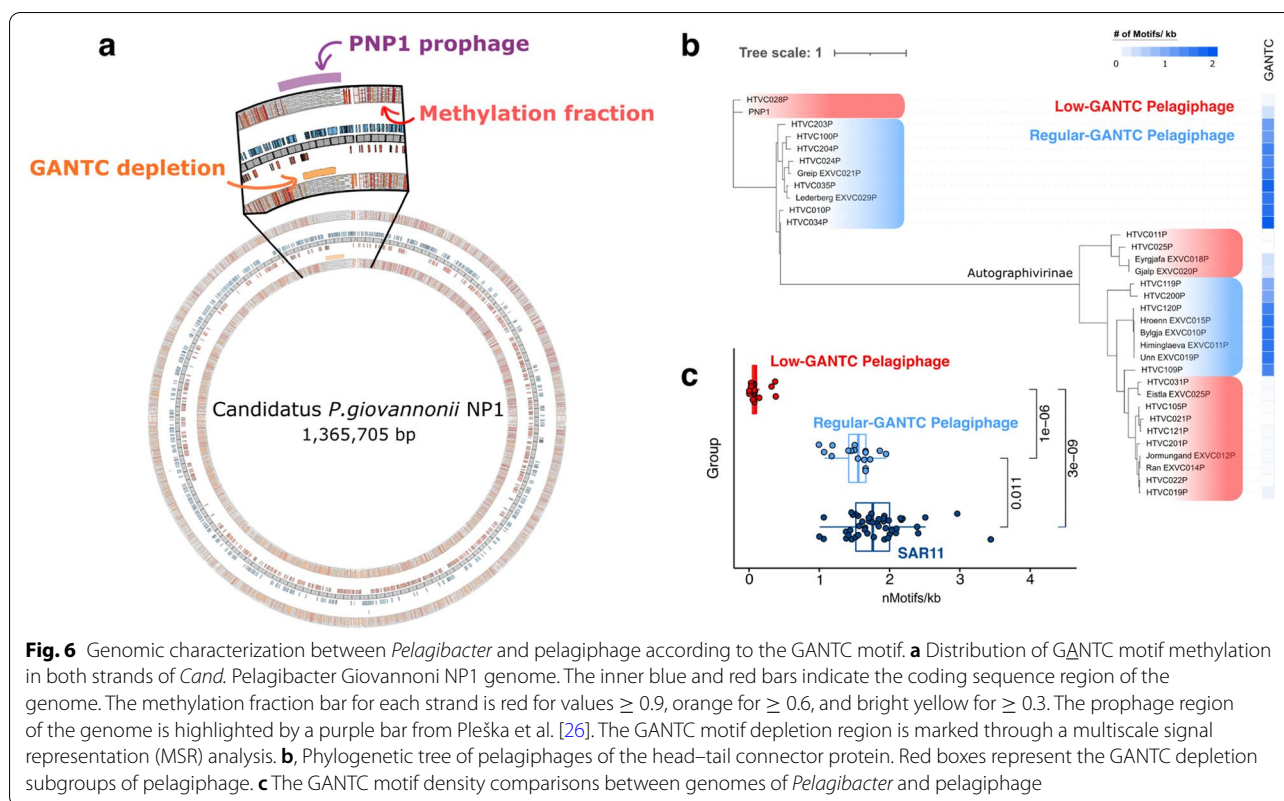


**Fig. 5** (See legend on previous page.)



RM system was not, as most were formed by orphan MTases without cognate REases. Unlike the other types, the type II RM system is known as a key strategic defense system of prokaryotes against diverse invasive foreign DNA (e.g., plasmids or phages) because the recognition sites of MTase and REase are specifically similar [28]. Particularly, type II RM systems have constant opportunities for genetic transfer through horizontal gene transfer and homologous recombination [29], and also exhibit subsequent additive characteristics that can be selfishly transmitted in populations [30]. Among them, only MTase, not REase, typically remained an orphan, which may be explained by the degradation or inactivation of congruent REase after the acquisition of the RM system by horizontal acquisition [31, 32]. In particular, the loss of one component from a horizontally-acquired type II RM system may be driven by the selective pressure of genomic streamlining in the pelagic environment. Alternatively, as part of a horizontal gene transfer process of the RM system, MTase may be transferred before REase to protect host DNA from cleavage [33]. Regardless of the underlying mechanisms, it appears that type II MTases are much more frequently detected as orphan MTases in the SHIPPO dataset. In these cases of orphan MTase, DNA methylation is likely to be used to as regulator of cellular

mechanisms rather than as defense mechanisms of exogenous invasive DNA, because this latter role would require the REase component.

After investigating the potential roles of methylation globally, we next studied the methylation patterns for the most dominant organism, *Pelagibacter*, in more detail. As mentioned above, the MTases of most marine microorganisms were found without counterpart REases, and conserved MTases were also observed without counterpart REases in the four *Pelagibacter* proMAGs. In particular, the *Pelagibacter* proMAGs showed that the methylated motif (GANTC) and the recognition motif of their MTase were consistent. The GANTC motif in the *Pelagibacter* proMAGs was globally uniformly distributed throughout the genome (Shapiro–Wilk test: genic  $> 0.05$ , intergenic  $> 0.05$ , and regulatory  $> 0.05$ ). For bacterial MTases involved in gene regulation, methylated motifs are frequently located upstream of regulated genes [28]. In this study, we also found that GANTC was enriched in the intergenic region of *Pelagibacter*, indicating that GANTC favors an epigenetic role ( $P$  value = 0.05, Supplementary Figure S5).

Although most motifs are known to be methylated throughout prokaryotic genomes [16], some motif sites have been found that remain unmethylated [28, 34, 35]. These unmethylated sites may be due to competitive

binding between MTases and regulatory proteins due to epigenetic regulation [36, 37]. Therefore, as an epigenetic role was expected from the GANTC distribution within *Pelagibacter* proMAG (SHIPPO\_PRO\_33), the methylation status of different GANTC loci in this genome was explored to identify potential epigenetic unmasking [17, 28]. Overall, unmethylated GANTC motifs were observed across multiple stations and loci (Fig. 4a, b). Particularly, samples from St6, 8, and 9 showed a higher number of unmethylated sites, which lacked a clear explanation when considering the geographic, temperature, and salinity gradient in the dataset. Understanding the epigenetic regulation of all GANTC loci in a genome-wide manner remains an important challenge. However, combining metatranscriptomics and metaproteomics with environmental metadata in a larger dataset may help to further elucidate these mechanisms. Across the SHIPPO dataset, the only GANTC positions that were broadly unmethylated were observed in intergenic and likely regulatory regions, including regions upstream of the *sufE* (K04488) gene from the Suf (sulfur-forming) system. This gene is part of the SufSE complex with *sufS* and is involved in the transport of sulfur to the sulfur mobilization protein. Along with *sufS*, this gene was also significantly more highly expressed in the absence of dimethylsulfoniopropionate (DMSP) in sulfur-limited conditions in the laboratory [38]. We also observed unmethylated GANTC in the regulatory region of *groEL* (chaperone gene, K04077), which is also more highly expressed in sulfur-restricted conditions [38]. Furthermore, because proteins are constantly being degraded due to exposure to environmental stresses, metaproteomics revealed that *groEL* of SAR11 was among the most abundant proteins on the ocean surface, and *groEL* genes are thus likely to be highly expressed [39]. Moreover, based on previously published data, we found that most GANTC motifs (99.86%, 3477/3482) were fully methylated (both strands were methylated) under DMSP-rich laboratory culture conditions of *Candidatus Pelagibacter Giovanni* NP1 [23], which is most closely related to SHIPPO\_PRO\_33 (ANI  $\geq$  92.36). *Candidatus Pelagibacter ubique*, which harbors a streamlined genome, typically requires a source of exogenous reduced sulfur compounds such as DMSP for growth [26]. Natural DMSP levels in the surface seawater range from 1 to 100 nM [40–42], which constitutes a significantly oligotrophic environment relative to DMSP-rich laboratory conditions (10  $\mu$ M) for culturing *Pelagibacter*. Therefore, the differences in unmethylated GANTCs between environmental and laboratory settings may reflect the methylation-based epigenetic regulation of nutrient acquisition.

Viruses primarily use DNA methylation to counter host defense systems, such as the RM system, although

some also exploit methylation to signal a transition in their status from a latent to a lytic state [43]. The methylation of viral DNA is also inherently transient as it is either derived from viral-encoded MTase or the host's MTase and can be demethylated via passage through an MTase-free host. Viruses most often use their own MTases as a counter-defense and as a signal to initiate lysis state and DNA packaging [44, 45]; however, incongruences were observed in our study between the methylome of the viral genome and the recognition motif of the predicted MTase. Therefore, DNA methylation of the viral genome in the marine environment is most likely a marker left behind from a previous host, rather than driven by virus-encoded MTases. To support the hypothesis, we further analyzed the DNA methylomes of the viral genomes detected at multiple sampling stations, and confirmed that methylation patterns and loci differ between geographic locations for individual viruses (Fig. 5c). Although further studies are needed to understand the biological and ecological significance of DNA methylation in viruses in the real world, an explanation for our results is that a substantial amount of methylation in virus genomes derive from their host machinery, and different hosts altered the virus methylome with MTases that recognize different motifs.

Finally, we noticed that in the eight proMAGs of the SHIPPO catalog spanning the order Pelagibacterales, their genomes lacked all genes associated with typical phage defense mechanisms including CRISPR and RM systems. Consistent with our results, there have not been previously reported RM systems in the SAR11 genome, except for a few common defense systems on some SAR11 genomes [46]. Despite the absence of identifiable RM system in our SHIPPO *Pelagibacterales* proMAGs, we did observe a clear GANTC density bias in the genome of some known pelagiphage clades. This raises the possibility that methylation marks may have been used as anti-phage defense in the past, or that some strains within or related to the SAR11 clade do use RM systems as phage defense, in which case the difference in GANTC frequency would be related to differences in host range between phage clades.

## Conclusion

Genome-centric metagenomics leverages reconstructed genomes spanning multiple kingdoms—including viruses, prokaryotes, and eukaryotes—to investigate the biological processes occurring in natural microbial communities. Here, we analyzed community-wide and single-nucleotide level epigenetics in the oceanic microbial communities, and the approach proposed herein provides a roadmap for how to analyze DNA methylome changes across different environments. Additionally,

successful genome reconstruction using long- and short-reads allowed for the inference of phage-host-related methylation and co-evolutionary histories. Overall, our findings illustrate how genome-wide epigenetic analysis and phage-host-related methylation, along with the establishment of global metagenome-methylation databases, can help characterize microbiomes.

## Methods

### Sample collection and shotgun sequencing

Surface seawater samples (7 m depth) were collected at 10 stations (referred to here as St2–St11) along a transect of 44–63°N latitude (approximately 4000 km) in the northwest Pacific Ocean during the R/V *ARAON* cruise of the Korea Polar Research Institute (KOPRI) for a Shipborne Pole-to-Pole Observations (SHIPPO) project in July 2015 (Supplementary Figure S1 and Supplementary Table S1). Onboard, 20 L of seawater at each station was immediately filtered through a 147-mm GF/A glass microfiber filter (Whatman, Maidstone, UK) and subsequently through a 147-mm, 0.22- $\mu$ m membrane filter (Millipore, Billerica, USA) using a peristaltic pump. These filters were stored at -80°C until DNA extraction. The filters were chopped and dissolved in sucrose-Tris-EDTA buffer (STE buffer; 0.74 M sucrose, 1 M Tris pH 8.3, 0.5 M EDTA, and distilled water). Next, samples were treated with lysozyme (5 mg/mL Tris-HCl), followed by 10% SDS and proteinase K (20 mg/mL). Genomic DNA was extracted using a DNeasy Blood & Tissue Kit (QIAGEN, Hilden, Germany) following the manufacturer-provided protocol. Long-read shotgun sequencing was conducted using the Pacific Biosciences (PacBio) RSII sequencing system (Menlo Park, CA, USA) with P6-C4 chemistry at DNA Link (Seoul, Korea) according to the MagBead OneCellPerWell v1 protocol. Each DNA sample was sequenced in continuous long-reading (CLR) mode with a library size of 5 kb, and three single-molecule real-time (SMRT) cells were used per sample (a total of 32.2 Gb was generated with read average of 797.9 bp length). In addition, for short-read shotgun sequencing, libraries were constructed by TruSeq Nano and sequenced using an Illumina HiSeq 4000 system with paired-end reads (a total of 154.4 Gb was generated with read average of 151 bp length) at Macrogen (Seoul, Korea).

### Read preprocessing and contig assembly

Short-reads were preprocessed with FaQCs (v. 2.09; the default option with *-q* 20) [47], and a duplicated read removal process was performed using FastUniq [48]. Quality-filtered reads of each sample were assembled into contigs using MEGAHIT (v. 1.1.3) [49] in “meta-sensitive” mode. In addition, reads of all 10 samples were assembled into contigs through co-assembly with the same options as above.

Long-reads were preprocessed with a hybrid error correction approach using FM-index Long Read Corrector (FMLRC; v. 1.0.0) [50] with quality-filtered short-reads. After preprocessing, corrected long-reads of each sample were assembled using Flye (v. 2.4.1) [51] with “meta-Flye” and “PacBio corrected reads” options. Co-assembly was also performed on all 10 samples with the same options as above. Furthermore, assembled contigs from long-reads were polished using Pilon (v. 1.23) [52] twice.

### Genome binning of the northwest Pacific Ocean

Contig coverage was calculated using only short reads, which consisted of a uniform length (151 bp) with the Burrows-Wheeler Aligner tool (BWA-MEM v. 0.7.17) [53]. Next, contigs from individual assembly and co-assembly were binned separately using CONCOCT (v. 0.5.0) [54] and MetaBAT (v. 2.12.1) [55], respectively. Additionally, a manual binning process was performed with mmgenome2 (<https://github.com/KasperSkytte/mmgenome2>). Then, these bins were refined by the integrative *k*-means clustering approach (ACR: <https://github.com/hoonjeseong/acr>) using contig coverages.

For prokaryotes, the quality of genome bins was estimated using CheckM [56]. Only bins with better than medium quality (completeness > 50% and contamination < 10%) [8] were referred for metagenome-assembled genomes (MAGs) and used for further analysis. All MAGs were dereplicated at 99% average nucleotide identity (ANI) value using dRep [57] with the options “-comp 50-con 10” and then dRep was re-run with “-sa 0.95” (95% ANI value clustering) to screen representative species MAGs. To improve the quality of short- and long-read sequencing, a reassembly process was performed on only high-quality MAGs (HQ MAGs, completeness > 90% and contamination < 5%). Quality-filtered short- and long-reads were mapped against HQ MAGs using bowtie2 [58] and PBAAlign (<https://github.com/PacificBiosciences/pbalign>). Then, mapped reads were retrieved using “samtools view” with *-f* 65, *-f* 129, and *-F* 4 options for forward, reverse, and unpaired long reads, respectively [59]. Each HQ MAG was reassembled with the hybrid assembly approach using Unicycler [60]. The obtained prokaryotic MAGs (referred to as SHIPPO PRO MAG) were designated as SHIPPO\_PRO\_XX and classified using the Genome Taxonomy Database Toolkit (GTDB-Tk) [11]. The phylogenetic tree was constructed by PhyloPhlAn2 [61] and visualized by iTOL v. 6 [62].

For eukaryotes, eukaryotic bin classification was performed for those > 5 Mb in size by EukRep [63]. Afterward, a detailed quality evaluation was performed through EukCC [64], and eukaryotic MAGs were selected according to the criteria of “Completeness-5\*Contamination > 50.” In addition, the MAG with

the highest score (Completeness-5\*Contamination + 0.5\*log(N50)) in the group within ~99% of the ANI value was selected as the representative eukaryotic MAG. Furthermore, species-level eukaryotic MAGs were chosen by the highest scores within ~95% ANI cluster. The eukaryotic MAGs (referred to as SHIPPO EUK MAG) were designated as SHPPO\_EUK\_XX, and their taxonomy was classified by phylogenetic topology with MAGs from Delmont *et al.* [65]. Phylogenetic analysis was processed with two DNA-dependent RNA polymerase (RNAP-a and RNAP-b) subunits. The concatenated protein sequences of RNAP-a and -b were aligned by MAFFT alignment (v. 7.402, FFT-NS-i algorithm with default option) [66], and gap sequences were trimmed using trimAl (v. 1.4) [67] with the parameter -gt 50. The phylogenetic trees were calculated by IQ-TREE (v. 1.6.12) [68] using the following parameters: -m LG + F + R10 -alrt 1000 -bb 1000; LG + F + R10 model, 1,000 replication of the Shimodaira-Hasegawa (SH)-like approximation likelihood ratio (aLRT) and ultrafast bootstrap approximation (UFBoot) [69].

The viral contigs were detected using VirSorter (only categories 1, 2, and 3) [70] and the Earth's Virome protocol [71] from all contigs through individual and co-assemblies. CD-HIT-EST [72] clustering was processed with 99% identity to remove duplicate viral contigs, and only > 5 kb contigs were subsequently used. Then, viral sequences were clustered as "population" with 95% ANI, which are currently defined as species-level taxonomy in viruses (viral operational taxonomic units: vOTUs)—via all-vs.-all pairwise BLASTn [73] using previous viral genome datasets (the Earth's Virome protocol [74] and the Global Ocean Viromes 2.0; GOV2.0 [75]). vOTUs were clustered with 95% identity across ≥80% aligned fraction, and at least one hit > 1 kb in length. Groups with previous study datasets were designated as vOTU\_XX, groups of two or more viral contigs only in the SHIPPO set were designated vOTU\_N\_XX, and singletons were designated vOTU\_sg\_XX (referred to as SHIPPO vOTU). For giant viruses, dereplicated viral contigs were binned using MetaBAT2 and filtered using NCLDV\_detector. Then, giant viral bins were further filtered with the same conditions as in Schulz *et al.* [76] through the quality assessment using the copy number of NCOVGs. These giant viral MAGs (referred to as SHIPPO GV) were designated as vOTU\_GV\_XX. Their ANI values were compared and then selected for representative strain- and species-level genomes with the completion and duplication ratio of NCOVGs. Next, the quality of vOTUs was assessed using CheckV [77] and divided into four groups: "complete" (0.02%,  $n = 4$ ), "high quality" (2.15%,  $n = 415$ ), "medium quality" (5.45%,  $n = 1052$ ) and "low

quality" (92.02%,  $n = 17,758$ ). Taxonomic classification of vOTUs was assigned by Demovir (<https://github.com/feargalr/Demovir>) with the comparison of amino acid sequence homologies to a viral subset of the TrEMBL database. Phylogenetic analyses were processed based on the Dice distance using sequence similarity comparisons of each contig using all-vs.-all tBLASTx (≥30% identity, ≥30 amino acids, and an e-value ≤0.01). The Dice distance between contigs A and B ( $D_{A,B}$ ) was calculated as  $1 - (2 \times AB/AA + BB)$ , where AB is the bit-score sum of all hits between genomes A and B. AA and BB are the bit-score sums of all hits from genomes A and B, respectively, compared to themselves. Then, we obtained a phylogenetic tree from the distance matrix via a neighbor-joining algorithm.

A total of 252 dereplicated proMAGs (99% average nucleotide identity; ANI) with ≥ 50% completeness and < 10% contamination remained (average completeness:  $78.80 \pm 14.09$ , and contamination:  $2.76 \pm 2.37$ ), 105 originated from the individual binning and 147 from the co-assembly binning. Forty-seven had > 90% completeness and < 5% contamination (near-complete), of which only three were high-quality MAGs that fit the Minimum Information about a Metagenome-assembled Genome (MIMAG) criteria [78] including rRNA and tRNA.

#### ANI comparison with reference datasets

To ascertain the novelty of SHIPPO MAGs, we collected two genome databases that derived ocean metagenomics (the *Tara* Oceans survey [10] and the Global Ocean Reference Genomes Tropics survey; GORG-Tropics [11]) for comparison with our data. The quality of MAGs from *Tara* Oceans and single-cell assembled genomes (SAGs) from GORG-Tropics were assessed using CheckM [56]. Genomes that were not at least medium-quality were excluded from subsequent analysis. We calculated the ANI values of SHIPPO MAGs for 957 MAGs and 4741 SAGs, respectively. Intra- and inter-species boundaries were differentiated with 95% and 83% ANI values, respectively, as previously studied.

#### Sample mapping

Each short-read of a sample was subsampled at 49 million paired reads (minimum sequencing throughput among samples) and mapped to the SHIPPO MAGs using Bowtie2 (v. 2.3.4.3) [58] with "--very-sensitive" parameter in end-to-end mode. Additionally, to avoid overestimating the read alignment, we excluded reads whose alignments score was < -20 (tag AS:i). The percentage of mapped reads to SHIPPO MAGs (mappability) was calculated by dividing the aligned reads by subsamples (49 million) paired reads in each sample.

### Diversity calculation

To calculate species-level diversity, mapped reads to species-level SHIPPO MAG were further filtered with the read alignment identity ( $\geq 95\%$ ) using pysam. Macrodiversity was calculated using Shannon diversity by the skbio diversity Python module (<http://scikit-bio.org/>) for each sample. Before calculating species microdiversity, we observed how many positions within the genome were shared by all samples with sufficient read depth. We only used MAGs with shared mapping positions across all samples wider than 20% of the genome breadth (60% for the viral contig) with  $\geq 10$  read depth. Then, single nucleotide variants (SNVs) were called with the following command: “samtools mpileup -l [overlapped region bed file] -Ou -C 50 -Af [SHIPPO fasta] [bam files] | bcftools call -vm0 -v -o [output vcf],” where “[overlapped region bed file]” is the bed format of the overlapped region from read-mapping, “[SHIPPO fasta]” is the fasta file of species-level SHIPPO MAG sequence, “[bam files]” are all bam files that result from read mapping to SHIPPO MAG sequence, and “[output vcf]” is the output vcf file of variant information. Each SNV was considered single nucleotide polymorphism (SNP) loci by classical definition as having an alternative allele supported by a frequency  $> 1\%$  and at least four reads. The microdiversity (nucleotide diversity,  $\pi$ ) of each genome was calculated using an equation from Schloissnig et al. [79]. Furthermore, the fixed index ( $F_{st}$ )—a measure of the population differentiation between samples—was calculated by additional inter-sample nucleotide diversity calculations.

### Gene annotation (methyltransferase (MTase) and restriction enzyme (REase))

Gene predictions of prokaryotes, eukaryotes, and viruses of SHIPPO MAG were processed with GeneMarkS-2 (v. 1.09\_1.07\_lic) [80], GeneMark-ES [81], and Prodigal [82], respectively. We annotated the protein-coding sequences using GhostKOALA [83] to generate Kyoto Encyclopedia of Genes and Genomes orthology (KO) classification.

RMS pipeline identified the restriction-modification (RM) systems (<https://github.com/oliveira-lab/RMS>) using Hidden Markov model (HMM) profiles built from curated reference protein sequences by a type of RM system. In addition, genes related to the RM system were obtained by its type through KO terms, as follows:

- Type I RM system (K01153; type I REase, R subunit [EC:3.1.21.3], K01154; type I REase, S subunit [EC:3.1.21.3], K03427; type I REase M protein [EC:2.1.1.72])
- Type II RM system (K01155; type II REase [EC:3.1.21.4], K06223; DNA adenine methylase [EC:2.1.1.72], K13581; modification methylase [EC:2.1.1.72], K07317; adenine-specific DNA-MTase [EC:2.1.1.72], K07318; adenine-specific DNA-MTase [EC:2.1.1.72], K07319; adenine-specific DNA-MTase [EC:2.1.1.72], K00571; site-specific DNA-MTase (adenine-specific) [EC:2.1.1.72], K00558; DNA (cytosine-5)-MTase 1 [EC:2.1.1.37], K00590; site-specific DNA-MTase (cytosine-N4-specific) [EC:2.1.1.113])
- Type III RM system (K01156; type III REase [EC:3.1.21.5], K07316; adenine-specific DNA-MTase [EC:2.1.1.72])
- Type IV RM system (K07451; 5-methylcytosine-specific REase A [EC:3.1.21.-], K07452; 5-methylcytosine-specific REase B [EC:3.1.21.-], K19147; 5-methylcytosine-specific REase subunit McrC, K07448; restriction system protein)

The RM system type was classified by searching genes encoding the MTase and REase that were  $< 10$  genes apart.

### Host-prediction

We conducted multiple strategies for viral host prediction to identify potential microbial hosts of the vOTUs from SHIPPO MAG. (1) Sequence homology matches: SHIPPO vOTU genomes were aligned against SHIPPO PRO MAG using BLASTn. Among the best hits, hits that met the criterion of  $\geq 75\%$  identity with alignment length  $\geq 2500$  bp were considered. (2) Clustered Regularly Interspaced Short Palindromic Repeats (CRISPR) spacer matches: CRISPR spacers were identified using CRT (CLI v. 1.2) [84] and PILER-CR (v. 1.06) [85] using the criteria established in the Microbial Genome Annotation Pipeline (MiGAP v. 4) [86]. Spacer sequences were compared by all-vs.-all BLASTn with “-task BLASTn-short -evaluate 1e-10-perc\_identity 95” parameters. (3) tRNA matches: transporter RNAs were obtained using ARAGORN (v. 1.2.38) [87] and compared by all-vs.-all BLASTn with “-perc\_identity 100” parameter. Only BLAST hits were considered with 100% coverage query length of the alignment. We matched the host of SHIPPO vOTU against SHIPPO PRO MAG through the filtered results from the three abovementioned strategies.

### DNA modification and motif detection

DNA methylation was detected with a series of pipelines from BaseMod (<https://github.com/ben-lerch/BaseMod-3.0>). Briefly, each long-read of samples was mapped to the SHIPPO MAG sequences using PBAAlign. Then, the modified positions of genomes were identified through ipdSummary (v. 2.0), which is a *t* test based comparison of interpulse duration ratios (IPDs) to the “synthetic

control” model. These approaches used the same parameters documented in BaseMode. To find novel motifs methylated from each SHIPPO MAG, we found methylated sequence motifs by a de novo approach using MultiMotifMaker [14]. Additionally, we collected the previously curated recognition motifs of MTase from the Restriction Enzyme Database (REBASE; <http://rebase.neb.com/cgi-bin/msublist>) [13] to further capture methylated motifs in SHIPPO MAG.

### Meta-epigenomic analysis

Due to the specificity of the metagenome, insufficient reads were sequenced to calculate methylation for all SHIPPO MAGs. Therefore, using a relatively weak criterion of  $10\times$  coverage per strand and  $\geq 30$  modification quality value, we identified the overall  $N^6$ -methyladenosine ( $m^6A$ ) and  $N^4$ -methylcytosine ( $m^4C$ ) DNA modification trends throughout SHIPPO MAGs across the kingdoms of life. To complement this point, the ratio of methylated motifs for each genome in each sample was calculated only within a genomic breadth of coverage in  $10\times$ . Additionally, when the genome breadth of coverage was less than a certain percentage of each MAG size (SHIPPO PRO < 20%, SHIPPO EUK < 10%, SHIPPO vOTU < 60%, SHIPPO GV < 20%; according to genome size), they were excluded from further analysis.

MTase sequences were downloaded from REBASE (<http://rebase.neb.com/cgi-bin/msubprolist>), and the most similar MTase was searched for by querying the candidate MTase of SHIPPO MAG with a  $\geq 50\%$  identity parameter using BLASTp in REBASE. Afterward, we compared the motifs obtained from the methylation analysis of SMRT (which were > 20% methylated) sequencing with the recognition motif of the most similar reference MTase.

### Genome-wide epigenetic analysis

To compare DNA methylation profiles at single-nucleotide resolution across samples, we selected the most dominant MAGs (SHIPPO\_PRO\_33) that mapped  $\geq 50\%$  of the genomic breadth of  $20\times$  per strand in all samples. MAGs consist of fractionated genomes, making it difficult to understand the overall genomic structure, so we rearranged the order of the contigs through genome comparison with the closest reference genome using the Mauve Contig Mover [88]. Then, the replication origin (*ori*) and terminus (*ter*) were identified using the *gc\_skew.py* script (<https://github.com/christophertbro wn/iRep>) through the concatenate reordered contigs. In addition, methylation fractions (cellular fractions of DNA methylation) in regions overlapped by  $20\times$  in all samples were compared at the single nucleotide level.

### Motif enrichment

Motif enrichment analysis was processed by calculating the motif densities of three regions: regulatory, genic, and intergenic. Five hundred simulations were performed by shuffling the coding region based on the average gene length and the number of genes present in each genome strand, and the Shapiro test ( $P$  value > 0.05) was performed for each of the three regions. Next,  $z$ -scores were calculated for the motifs following normality and converted into  $p$ -values. Moreover, we used a multiscale signal representation (MSR) [89] method to assess whether the motif for specific regions is enriched or depleted (“section\_2” of <https://github.com/oliveira-lab/BEAST>).

### Principal coordinate analysis (PCoA)

PCoA was performed based on the SNVs, methylated motifs, and methylation fractions across samples with the Bray–Curtis distance with R package “vegan” and visualized with “ggplot2”.

### Abbreviations

MTase: Methyltransferase; RM: Restriction–modification; REase: Restriction enzyme; SMRT: Single-molecule real-time;  $m^6A$ :  $N^6$ -methyladenosine;  $m^5C$ :  $N^5$ -methylcytosine; SHIPPO: Shipborne Pole-to-Pole Observations; PacBio: Pacific Biosciences; MAG: Metagenome-assembled genome; MIMAG: Minimum Information about a Metagenome-assembled Genome; GORG-Tropics: Global Ocean Reference Genomes Tropics; GTDB: Genome Taxonomy Database; REBASE: Restriction Enzyme database; *FST*: Fixation index; *IPD*: Interpulse duration; *SNMV*: Single nucleotide methylation variation; *SNV*: Single nucleotide variant; *ori*: Replication origin; *ter*: Replication terminus; vOTUs: Viral operational taxonomic units; PCoA: Principal coordinate analysis.

### Supplementary Information

The online version contains supplementary material available at <https://doi.org/10.1186/s40168-022-01340-w>.

**Additional file 1: Supplementary Figure S1.** SHIPPO samples in the northwest Pacific Ocean. **Supplementary Figure S2.** Compositional profile of microbial communities spanning eukaryotes, prokaryotes, and viruses. **Supplementary Figure S3.** The *Cand. P. Giovannoni* NP1 genome-wide distribution of methylated fractions. **Supplementary Figure S4.** The *Pelagibacter* (SHIPPO PRO 33) genome-wide distribution of methylated fractions. **Supplementary Figure S5.** GANTC motif density in the SHIPPO\_PRO\_33 genome. **Supplementary Figure S6.** Phylogenetic tree of eukaryotic plankton MAGs obtained from SHIPPO. **Supplementary Figure S7.** The GANTC methylation proportion comparison according to the genome fraction in six species belonging to the Alphaproteobacteria. **Supplementary Figure S8.** Benchmarking of viral taxonomy classification according to the number and fraction of viral genes. **Supplementary Table S1.** SHIPPO samples in the northwest Pacific Ocean. **Supplementary Table S2.** Methylated motifs of SHIPPO MAGs. **Supplementary Table S3.** Unmethylated GANTC sites across samples.

**Additional file 2: Supplementary Data 1.** Genome information of SHIPPO MAGs. **Supplementary Data 2.** (DOI link: <https://doi.org/10.6084/m9.figshare.17161715>). Genome files of SHIPPO MAGs.

**Additional file 3: Supplementary Data 3.** RM system of MAGs from ocean metagenomic studies.

**Additional file 4: Supplementary Data 4.** Methylation profiles of 5-mer motifs across MAGs and sampling stations.



### Authors' contributions

W.J.S. and H.J.S. conceptualized the study. C.Y.H. collected samples. H.J.S. analyzed and visualized the metagenomic and meta-epigenomic data and wrote the original draft. S.R. reviewing and editing the manuscript. All documents were read and approved by all authors.

### Funding

This research was supported by Basic Science Research Program through the National Research Foundation of Korea (NRF) funded by the Ministry of Education (NRF-2014R1A1A2A16055779), and by Ministry of Science and ICT (NRF-2017R1A2B4008968, NRF-2019R1A2C1090861). The U.S. Department of Energy Joint Genome Institute (S.R.) supported this work by the Office of Science of the U.S. Department of Energy under contract no. DE-AC02-05CH11231.

### Availability of data and materials

The raw Illumina and SMRT sequence files used in this study were deposited in the NCBI BioProject under the accession PRJNA784005. Genome files of SHIPPO MAGs are provided online at Figshare (Supplementary Data 2; <https://doi.org/10.6084/m9.figshare.17161715>). Analysis codes of the meta-epigenomics are available at the repository (<https://github.com/hoonjeseong/Meta-epigenomics>) under a MIT license.

### Declarations

#### Ethics approval and consent to participate

Not applicable.

#### Consent for publication

Not applicable.

#### Competing interests

The authors declare that they have no competing interests.

### Author details

<sup>1</sup>Department of Systems Biotechnology, Chung-Ang University, Anseong, Republic of Korea. <sup>2</sup>DOE Joint Genome Institute, Lawrence Berkeley National Laboratory, Berkeley, CA, USA. <sup>3</sup>School of Earth and Environmental Sciences and Research Institute of Oceanography, Seoul National University, Seoul, Republic of Korea.

Received: 22 January 2022 Accepted: 28 July 2022

Published: 28 September 2022

### References

- Vasu K, Nagaraja V. Diverse functions of restriction–modification systems in addition to cellular defense. *Microbiol Mol Biol Rev.* 2013;77:53–72.
- Sánchez-Romero MA, Casadesús J. The bacterial epigenome. *Nat Rev Microbiol.* 2020;18:7–20.
- Arber W. DNA modification and restriction. *Progress in nucleic acid research and molecular biology.* London: Academic; 1974. p. 1–37.
- De Ste CM, Vacca I, Kwun MJ, Ralph JD, Bentley SD, Haigh R, et al. Phase-variable methylation and epigenetic regulation by type I restriction–modification systems. *FEMS Microbiol Rev.* 2017;41:53–515.
- Tan A, Attack JM, Jennings MP, Seib KL. The capricious nature of bacterial pathogens: phasevariations and vaccine development. *Front Immunol.* 2016;7:586.
- Beaulaurier J, Schadt EE, Fang G. Deciphering bacterial epigenomes using modern sequencing technologies. *Nat Rev Genet.* 2019;20:157–72.
- Beaulaurier J, Zhu S, Deikus G, Mogno I, Zhang XS, Davis-Richardson A, et al. Metagenomic binning and association of plasmids with bacterial host genomes using DNA methylation. *Nat Biotechnol.* 2018;36:61–9.
- Tourancheau A, Mead EA, Zhang XS, Fang G. Discovering multiple types of DNA methylation from bacteria and microbiome using nanopore sequencing. *Nat Methods.* 2021;18:491–8.
- Hiraoka S, Okazaki Y, Anda M, Toyoda A, Nakano SI, Iwasaki W. Metaepigenomic analysis reveals the unexplored diversity of DNA methylation in an environmental prokaryotic community. *Nat Commun.* 2019;10:159.
- Delmont TO, Quince C, Shaiber A, Esen ÖC, Lee STM, Rappé MS, et al. Nitrogen-fixing populations of Planctomycetes and Proteobacteria are abundant in surface ocean metagenomes. *Nat Microbiol.* 2018;3:804–13.
- Pachiadaki MG, Brown JM, Brown J, Beuzidit O, Berube PM, Biller SJ, et al. Charting the complexity of the marine microbiome through single-cell genomics. *Cell.* 2019;179:1623–35.
- Parks DH, Chuvochina M, Chaumeil PA, Rinke C, Mussig AJ, Hugenholtz P. A complete domain-to-species taxonomy for Bacteria and Archaea. *Nat Biotechnol.* 2020;38:1079–86.
- Roberts RJ, Vincze T, Posfai J, Macelis D. REBASE—a database for DNA restriction and modification: enzymes, genes and genomes. *Nucleic Acids Res.* 2015;43:D298–9.
- Li T, Zhang X, Luo F, Wu FX, Wang J. MultiMotifMaker: a multi-thread tool for identifying DNA methylation motifs from Pacbio reads. *IEEE/ACM Trans Comput Biol Bioinform.* 2020;17:220–5.
- Zhu S, Beaulaurier J, Deikus G, Wu TP, Strahl M, Hao Z, et al. Mapping and characterizing N6-methyladenine in eukaryotic genomes using single-molecule real-time sequencing. *Genome Res.* 2018;28:1067–78.
- Wion D, Casadesús J. N6-methyl-adenine: an epigenetic signal for DNA–protein interactions. *Nat Rev Microbiol.* 2006;4:183–92.
- Oliveira PH, Ribis JW, Garrett EM, Trzilova D, Kim A, Sekulovic O, et al. Epigenomic characterization of *Clostridioides difficile* finds a conserved DNA methyltransferase that mediates sporulation and pathogenesis. *Nat Microbiol.* 2020;5:166–80.
- Fang G, Munera D, Friedman DI, Mandlik A, Chao MC, Banerjee O, et al. Genome-wide mapping of methylated adenine residues in pathogenic *Escherichia coli* using single-molecule real-time sequencing. *Nat Biotechnol.* 2012;30:1232–9.
- Srikhanta YN, Gorrell RJ, Steen JA, Gawthorne JA, Kwok T, Grimmond SM, et al. Phasevarion mediated epigenetic gene regulation in *Helicobacter pylori*. *PLoS One.* 2011;6:e27569.
- Casadesús J, Low DA. Programmed heterogeneity: epigenetic mechanisms in bacteria. *J Biol Chem.* 2013;288:13929–35.
- Manso AS, Chai MH, Attack JM, Furi L, De Ste CM, Haigh R, et al. A random six-phase switch regulates pneumococcal virulence via global epigenetic changes. *Nat Commun.* 2014;5:5055.
- Zweiger G, Marczynski G, Shapiro L. A *Caulobacter* DNA methyltransferase that functions only in the predivisional cell. *J Mol Biol.* 1994;235:472–85.
- Morris RM, Cain KR, Hvorecny KL, Kollman JM. Lysogenic host–virus interactions in SAR11 marine bacteria. *Nat Microbiol.* 2020;5:1011–5.
- Reisenauer A, Kahng LS, McCollum S, Shapiro L. Bacterial DNA methylation: a cell cycle regulator? *J Bacteriol.* 1999;181:5135–9.
- Wilson WH, Van Etten JL, Allen MJ. The *Phycodnaviridae*: the story of how tiny giants rule the world. *Curr Top Microbiol Immunol.* 2009;328:1–42.
- Tripp HJ, Kitner JB, Schwalbach MS, Dacey JW, Wilhelm LJ, Giovannoni SJ. SAR11 marine bacteria require exogenous reduced sulphur for growth. *Nature.* 2008;452:741–4.
- Oliveira PH, Touchon M, Rocha EPC. The interplay of restriction–modification systems with mobile genetic elements and their prokaryotic hosts. *Nucleic Acids Res.* 2014;42:10618–31.
- Blow MJ, Clark TA, Daum CG, Deutschbauer AM, Fomenkov A, Fries R, et al. The epigenomic landscape of prokaryotes. *PLoS Genet.* 2016;12:e1005854.
- Oliveira PH, Touchon M, Rocha EP. Regulation of genetic flux between bacteria by restriction–modification systems. *Proc Natl Acad Sci U S A.* 2016;113:5658–63.
- Kobayashi I. Behavior of restriction–modification systems as selfish mobile elements and their impact on genome evolution. *Nucleic Acids Res.* 2001;29:3742–56.
- Lin LF, Posfai J, Roberts RJ, Kong H. Comparative genomics of the restriction–modification systems in *Helicobacter pylori*. *Proc Natl Acad Sci U S A.* 2001;98:2740–5.
- Seshasayee ASN, Singh P, Krishna S. Context-dependent conservation of DNA methyltransferases in bacteria. *Nucleic Acids Res.* 2012;40:7066–73.
- Jeltsch A, Pingoud A. Horizontal gene transfer contributes to the wide distribution and evolution of type II restriction–modification systems. *J Mol Evol.* 1996;42:91–6.
- Hale WB, van der Woude M, Low DA. Analysis of nonmethylated GATC sites in the *Escherichia coli* chromosome and identification of sites that are differentially methylated in response to environmental stimuli. *J Bacteriol.* 1994;176:3438–41.

35. Tavazoie S, Church GM. Quantitative whole-genome analysis of DNA-protein interactions by in vivo methylase protection in *E. coli*. *Nat Biotechnol*. 1998;16:566–71.
36. Lim HN, van Oudenaarden A. A multistep epigenetic switch enables the stable inheritance of DNA methylation states. *Nat Genet*. 2007;39:269–75.
37. Ardisson S, Redder P, Russo G, Frandi A, Fumeaux C, Patrignani A, et al. Cell cycle constraints and environmental control of local DNA hypomethylation in  $\alpha$ -proteobacteria. *PLoS Genet*. 2016;12:e1006499.
38. Smith DP, Nicora CD, Carini P, Lipton MS, Norbeck AD, Smith RD, et al. Proteome remodeling in response to sulfur limitation in "*Candidatus Pelagibacter ubique*". *mSystems*. 2016;1:e00068–16.
39. Sowell SM, Wilhelm LJ, Norbeck AD, Lipton MS, Nicora CD, Barofsky DF, et al. Transport functions dominate the SAR11 metaproteome at low-nutrient extremes in the Sargasso Sea. *ISME J*. 2009;3:93–105.
40. Jarníková T, Dacey J, Lizotte M, Levasseur M, Tortell P. The distribution of methylated sulfur compounds, DMS and DMSP, in Canadian subarctic and Arctic marine waters during summer 2015. *Biogeosciences*. 2018;15:2449–65.
41. Cui Y, Suzuki S, Omori Y, Wong SK, Ijichi M, Kaneko R, et al. Abundance and distribution of dimethylsulfoniopropionate degradation genes and the corresponding bacterial community structure at dimethyl sulfide hot spots in the tropical and subtropical Pacific ocean. *Appl Environ Microbiol*. 2015;81:4184–94.
42. Bürgermeister S, Zimmermann RL, Georgii HW, Bingemer HG, Kirst GO, Janssen M, et al. On the biogenic origin of dimethylsulfide: relation between chlorophyll, ATP, organismic DMSP, phytoplankton species, and DMS distribution in Atlantic surface water and atmosphere. *J Geophys Res Atmos*. 1990;95:20607–15.
43. Hoelzer K, Shackelton LA, Parrish CR. Presence and role of cytosine methylation in DNA viruses of animals. *Nucleic Acids Res*. 2008;36:2825–37.
44. Sternberg N, Coulby J. Cleavage of the bacteriophage P1 packaging site (pac) is regulated by adenine methylation. *Proc Natl Acad Sci U S A*. 1990;87:8070–4.
45. Murphy J, Mahony J, Ainsworth S, Nauta A, van Sinderen D. Bacteriophage orphan DNA methyltransferases: insights from their bacterial origin, function, and occurrence. *Appl Environ Microbiol*. 2013;79:7547–55.
46. Giovannoni SJ. SAR11 bacteria: the most abundant plankton in the oceans. *Annu Rev Mar Sci*. 2017;9:231–55.
47. Lo CC, Chain PS. Rapid evaluation and quality control of next generation sequencing data with FaQCs. *BMC Bioinform*. 2014;15:1–8.
48. Xu H, Luo X, Qian J, Pang X, Song J, Qian G, et al. FastUniq: a fast de novo duplicates removal tool for paired short reads. *PLoS One*. 2012;7:e52249.
49. Li D, Liu CM, Luo R, Sadakane K, Lam TW. MEGAHIT: an ultra-fast single-node solution for large and complex metagenomics assembly via succinct de Bruijn graph. *Bioinformatics*. 2015;31:1674–6.
50. Wang JR, Holt J, McMillan L, Jones CD. FMLRC: Hybrid long read error correction using an FM-index. *BMC Bioinform*. 2018;19:1–11.
51. Kolmogorov M, Bickhart DM, Behsaz B, Gurevich A, Rayko M, Shin SB, et al. metaFlye: scalable long-read metagenome assembly using repeat graphs. *Nat Methods*. 2020;17:1103–10.
52. Walker BJ, Abeel T, Shea T, Priest M, Abouelliel A, Sakthikumar S, et al. Pilon: an integrated tool for comprehensive microbial variant detection and genome assembly improvement. *PLoS one*. 2014;9(11):112963.
53. Li H. Aligning sequence reads, clone sequences and assembly contigs with BWA-MEM. *arXiv*. 2013;1303:3997.
54. Alneberg J, Bjarnason BS, De Bruijn I, Schimer M, Quick J, Lahti UZ, et al. Binning metagenomic contigs by coverage and composition. *Nat Methods*. 2014;11:1144–6.
55. Kang DD, Li F, Kirton E, Thomas A, Egan R, An H, et al. MetaBAT 2: an adaptive binning algorithm for robust and efficient genome reconstruction from metagenome assemblies. *PeerJ*. 2019;7:e7359.
56. Parks DH, Imelfort M, Skennerton CT, Hugenholtz P, Tyson GW. CheckM: assessing the quality of microbial genomes recovered from isolates, single cells, and metagenomes. *Genome Res*. 2015;25:1043–55.
57. Olm MR, Brown CT, Brooks B, Banfield JF. dRep: a tool for fast and accurate genomic comparisons that enables improved genome recovery from metagenomes through de-replication. *ISME J*. 2017;11:2864–8.
58. Langmead B, Salzberg SL. Fast gapped-read alignment with Bowtie 2. *Nat Methods*. 2012;9:357–9.
59. Li H, Handsaker B, Wysoker A, Fennell T, Ruan J, Homer N, et al. The sequence alignment/map format and SAMtools. *Bioinformatics*. 2009;25:2078–9.
60. Wick RR, Judd LM, Gorrie CL, Holt KE. Unicycler: resolving bacterial genome assemblies from short and long sequencing reads. *PLoS Comput Biol*. 2017;13:e1005595.
61. Asnicar F, Thomas AM, Beghini F, Mengoni C, Manara S, Manghi P, et al. Precise phylogenetic analysis of microbial isolates and genomes from metagenomes using PhyloPhlAn 3.0. *Nat Commun*. 2020;11:1–10.
62. Letunic I, Bork P. Interactive Tree Of Life (iTOL) v5: an online tool for phylogenetic tree display and annotation. *Nucleic Acids Res*. 2021;49:W293–6.
63. West PT, Probst AJ, Grigoriev IV, Thomas BC, Banfield JF. Genome-reconstruction for eukaryotes from complex natural microbial communities. *Genome Res*. 2018;28:569–80.
64. Saary P, Mitchell AL, Finn RD. Estimating the quality of eukaryotic genomes recovered from metagenomic analysis with EukCC. *Genome Biol*. 2020;21:244.
65. Delmont TO, Gaia M, Hinsinger DD, Fremont P, Vanni C, Guerra AF, et al. Functional repertoire convergence of distantly related eukaryotic plankton lineages revealed by genome-resolved metagenomics. *bioRxiv*. 2020;2021:10.
66. Katoh K, Standley DM. MAFFT multiple sequence alignment software version 7: improvements in performance and usability. *Mol Biol Evol*. 2013;30:772–80.
67. Capella-Gutiérrez S, Silla-Martínez JM, Gabaldón T. trimAl: a tool for automated alignment trimming in large-scale phylogenetic analyses. *Bioinformatics*. 2009;25:1972–3.
68. Nguyen LT, Schmidt HA, Von Haeseler A, Minh BQ. IQ-TREE: a fast and effective stochastic algorithm for estimating maximum-likelihood phylogenies. *Mol Biol Evol*. 2015;32:268–74.
69. Minh BQ, Nguyen MAT, von Haeseler A. Ultrafast approximation for phylogenetic bootstrap. *Mol Biol Evol*. 2013;30:1188–95.
70. Roux S, Enault F, Hurwitz BL, Sullivan MB. VirSorter: mining viral signal from microbial genomic data. *PeerJ*. 2015;3:e985.
71. Paez-Espino D, Pavlopoulos GA, Ivanova NN, Kyrpides NC. Nontargeted virus sequence discovery pipeline and virus clustering for metagenomic data. *Nat Protoc*. 2017;12:1673–82.
72. Li W, Godzik A. Cd-hit: a fast program for clustering and comparing large sets of protein or nucleotide sequences. *Bioinformatics*. 2006;22:1658–9.
73. Altschul SF, Gish W, Miller W, Myers EW, Lipman DJ. Basic local alignment search tool. *J Mol Biol*. 1990;215:403–10.
74. Paez-Espino D, Roux S, Chen IMA, Palaniappan K, Ratner A, Chu K, et al. IMG/VR v. 2.0: an integrated data management and analysis system for cultivated and environmental viral genomes. *Nucleic Acids Res*. 2019;47:D678–86.
75. Gregory AC, Zayed AA, Conceição-Neto N, Temperton B, Bolduc B, Alberti A, et al. Marine DNA viral macro- and microdiversity from pole to pole. *Cell*. 2019;177:1109–23.
76. Schulz F, Roux S, Paez-Espino D, Jungbluth S, Walsh DA, Denev VJ, et al. Giant virus diversity and host interactions through global metagenomics. *Nature*. 2020;578:432–6.
77. Nayfach S, Camargo AP, Schulz F, Eloe-Fadrosh E, Roux S, Kyrpides NC. CheckV assesses the quality and completeness of metagenome-assembled viral genomes. *Nat Biotechnol*. 2021;39:578–85.
78. Bowers RM, Kyrpides NC, Stepanauskas R, Harmon-Smith M, Doud D, Reddy TBK, et al. Minimum information about a single amplified genome (MISAG) and a metagenome-assembled genome (MIMAG) of bacteria and archaea. *Nat Biotechnol*. 2017;35:725–31.
79. Schloissnig S, Arumugam M, Sunagawa S, Mitreva M, Tap J, Zhu A, et al. Genomic variation landscape of the human gut microbiome. *Nature*. 2013;493:45–50.
80. Lomsadze A, Gemayel K, Tang S, Borodovsky M. Modeling leaderless transcription and atypical genes results in more accurate gene prediction in prokaryotes. *Genome Res*. 2018;28:1079–89.
81. Ter-Hovhannisyan V, Lomsadze A, Chernoff YO, Borodovsky M. Gene prediction in novel fungal genomes using an ab initio algorithm with unsupervised training. *Genome Res*. 2008;18:1979–90.
82. Hyatt D, Chen GL, LoCasio PF, Land ML, Larimer FW, Hauser LJ. Prodigal: prokaryotic gene recognition and translation initiation site identification. *BMC Bioinform*. 2010;11:1–11.

83. Kanehisa M, Sato Y, Morishima K. BlastKOALA and GhostKOALA: KEGG tools for functional characterization of genome and metagenome sequences. *J Mol Biol.* 2016;428:726–31.
84. Bland C, Ramsey TL, Sabree F, Lowe M, Brown K, Kyrpides NC, et al. CRISPR recognition tool (CRT): a tool for automatic detection of clustered regularly interspaced palindromic repeats. *BMC Bioinform.* 2007;8:1–8.
85. Edgar RC. PILER-CR: fast and accurate identification of CRISPR repeats. *BMC Bioinform.* 2007;8:1–6.
86. Huntemann M, Ivanova NN, Mavromatis K, Tripp HJ, Paez-Espino D, Palaniappan K, et al. The standard operating procedure of the DOE-JGI Microbial Genome Annotation Pipeline (MGAP v. 4). *Stand Genomic Sci.* 2015;10:1–6.
87. Laslett D, Canback B. ARAGORN, a program to detect tRNA genes and tmRNA genes in nucleotide sequences. *Nucleic Acids Res.* 2004;32:11–6.
88. Rissman AI, Mau B, Biehl BS, Darling AE, Glasner JD, Perna NT. Reordering contigs of draft genomes using the Mauve aligner. *Bioinformatics.* 2009;25:2071–3.
89. Knijnenburg TA, Ramsey SA, Berman BP, Kennedy KA, Smit AF, Wessels LF, et al. Multiscale representation of genomic signals. *Nat Methods.* 2014;11(6):689–94.

### Publisher's Note

Springer Nature remains neutral with regard to jurisdictional claims in published maps and institutional affiliations.

Ready to submit your research? Choose BMC and benefit from:

- fast, convenient online submission
- thorough peer review by experienced researchers in your field
- rapid publication on acceptance
- support for research data, including large and complex data types
- gold Open Access which fosters wider collaboration and increased citations
- maximum visibility for your research: over 100M website views per year

At BMC, research is always in progress.

Learn more [biomedcentral.com/submissions](https://biomedcentral.com/submissions)

